Controlled Synthesis of Fullerene-Attached Poly(3-Alkylthiophene)-Based Copolymers for Rational Morphological Design in Polymer Photovoltaic Devices

ARTICLE *in* MACROMOLECULES · AUGUST 2012

Impact Factor: 5.8 · DOI: 10.1021/ma300376m

Macromolecules

Article

pubs.acs.org/Macromolecules

Controlled Synthesis of Fullerene-Attached Poly(3-alkylthiophene)-Based Copolymers for Rational Morphological Design in Polymer Photovoltaic Devices

Shoji Miyanishi,[†] Yue Zhang,[‡] Kazuhito Hashimoto,*[,†,§] and Keisuke Tajima*[,†,§]

[†]Department of Applied Chemistry, School of Engineering, The University of Tokyo, 7-3-1 Hongo, Bunkyo-ku, Tokyo 113-8656, Japan

[‡]The Molecular Foundry and Advanced Light Source, Lawrence Berkeley National Laboratory, One Cyclotron Road, Berkeley, California 94720, United States

[§]HASHIMOTO Light Energy Conversion Project, ERATO, Japan Science and Technology Agency (JST), 7-3-1 Hongo, Bunkyo-ku, Tokyo 113-8656, Japan

Supporting Information

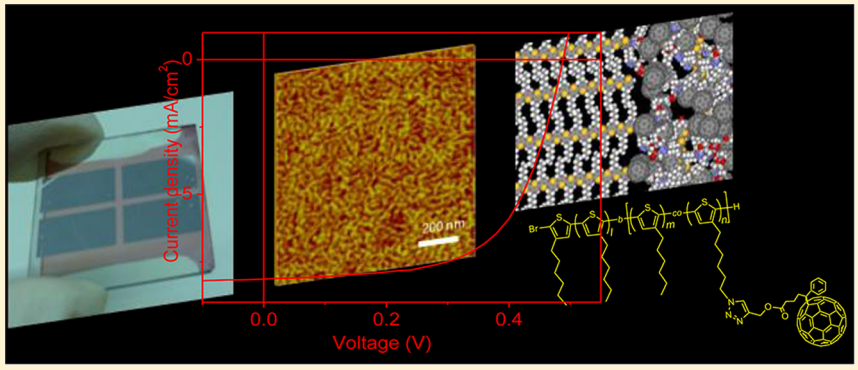

ABSTRACT: Poly(3-alkylthiophene)-based diblock copolymers with controllable block lengths were synthesized by combining the Grignard metathesis method, Ni-catalyzed quasi-living polymerization, and a subsequent azide−alkyne click reaction to introduce a fullerene functionality into the side chains of one of the blocks. The fullerene-attached copolymers had good solubility (>30 g L^{-1} in chlorobenzene) with high molecular weights (M_n > 20 000). The diblock copolymer films formed clear nanostructures with sizes of ca. 20 nm, driven by crystallization of the poly(3-hexylthiophene) block and aggregation of the fullerene groups, as observed in AFM phase images. The copolymer-based photovoltaic device showed a power conversion efficiency of 2.5%, with a much higher fill factor of 0.63 in comparison to the previously reported single component devices. These results indicate that rational material designs enable the construction of suitable donor−acceptor nanostructures for photovoltaic applications, without relying on the mixing of materials.

INTRODUCTION

Solution processable organic photovoltaic devices have recently received significant attention from the viewpoint of the application to a large area, flexible, and low cost electronic energy source.[1,2] The physical mixture of organic electron donor and acceptor materials, known as "bulk heterojunction", has been extensively studied to achieve high solar cell performance.[3,4] Owing to the limited exciton diffusion length in organic semiconductors (typically less than 10 nm), the construction of large donor/acceptor interfaces in the bulk heterojunction is necessary for efficient charge separation. At the same time, each donor and acceptor molecule must construct separate crystalline domains for subsequent charge transports. Therefore, controlling the donor and acceptor nanostructures by optimizing the mixing morphology is a mandatory procedure for achieving optimum performance in photovoltaic device materials.

However, because the mixing morphology is governed by the miscibility and solubility factors of the materials in a complicated manner, it is generally difficult to obtain suitable nanostructures by simple mixing. In fact, very few of the many semiconducting polymers give high device performance even with suitable energy levels, high charge mobility, and good light absorption properties probably because of the above-mentioned difficulty.[5,6] Furthermore, kinetically controlled morphology that relies on methods such as spin-coating of the mixed solutions could lead to problems in the reproducibility or

Received: February 23, 2012
Revised: June 15, 2012
Published: August 3, 2012

   dx.doi.org/10.1021/ma300376m | *Macromolecules* 2012, 45, 6424−6437

Scheme 1. Synthetic Route of Monomers and Fullerene Derivative

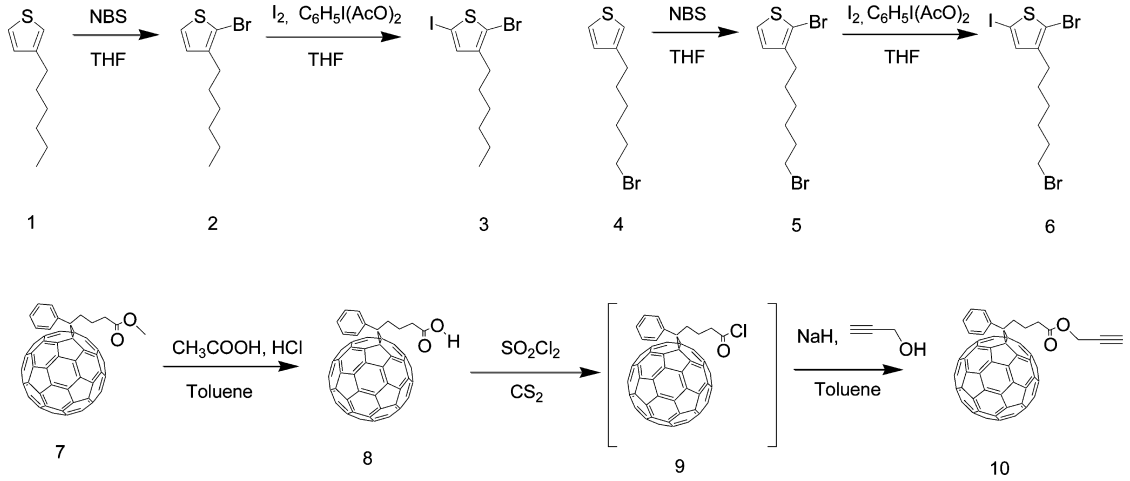

stability of the resulting morphology. This could be particularly important for the fabrication of large area devices and device stability.[7,8]

Recently, there have been reports of attempts to construct ordered nanostructures through self-organization of the molecules by using semiconducting oligomers[9−14] or copolymers with a covalently attached acceptor such as fullerene or perylenediimide derivatives.[15−22] These donor/acceptor connected systems have potential advantages over mixed bulk heterojunction systems in terms of precise morphological control and construction of thermodynamically stable nanostructures that can be fine-tuned by their molecular designs.[9,23,24]

The synthesis of such "all-in-one" semiconducting materials would be very desirable, but they currently face two major challenges. First, the performances of devices based on these types of materials have been much lower than those based on mixed bulk heterojunction. Covalent attachment guarantees close donor and acceptor group proximity and could lead to efficient charge separation and therefore to a higher short circuit current (J_{SC}) compared to mixed bulk heterojunction. However, fill factors (FF) of the devices are typically lower than 0.4, which are not as good for those of mixed bulk heterojunctions (~0.7). This difference could be because of the fact that the attachment of the donor and acceptors often prevents the construction of the separated donor/acceptor domains that work as charge transport paths.

The other challenge is the synthetic difficulty, especially in copolymer systems, because precise structural control of acceptor-attached copolymers could be a crucial factor in their application to photovoltaic devices. For example, contamination of unreacted components such as macroinitiators or free acceptor molecules should be carefully avoided because this could change the intrinsic morphological behavior of the copolymers. Lee et al. used the condensation reaction between fullerene derivatives and the polymer side chain to synthesize a soluble fullerene-attached rod−coil type block copolymer.[20] However, gel permeation chromatography (GPC) results showed that this polymer contained unreacted macroinitiators owing to incomplete reactions. The other groups used the Bingel or Prato reaction between C_{60} and the polymer side chain to obtain fullerene-attached diblock and random copolymers.[17,18] However, it is unclear whether the unreacted C_{60} is completely removed by Soxhlet extraction in hexane. In addition to these problems, side reactions must be carefully avoided during the attachment reaction. Hadziioannou et al. suggested that intra- and intermolecular cross-linking reactions during the attachment of acceptors could change polymer properties such as solubility.[19,25] Selective functionalization of C_{60} is especially difficult in fullerene chemistry owing to multiple functionality additions, which could lead to cross-linking and a significant decrease in the solubility.[26] Because the fullerene fraction of the molecules must be high enough for construction of electron conduction paths in the films (typically 33−50 wt % PCBM for P3HT:PCBM mixed bulk heterojunctions), a reaction with high yield and high selectivity for the fullerene attachment may be essential for obtaining soluble polymers applicable to photovoltaic devices.

Recently, we have reported preliminary results of the synthesis of regioregular poly(3-alkylthiphene)-based block and random copolymers with well-defined structures using the Grignard metathesis (GRIM) reaction and Ni-catalyzed quasi-living polymerization.[27] A fullerene derivative with an alkyne group was reacted with the alkyl azide side chains of the copolymers via Cu(I)-catalyzed click chemistry.[28,29] This reaction proceeds very efficiently and selectively under mild conditions with high durability to other functionalities, which makes it suitable for the synthesis of sterically hindered polymers.[26,30] It was shown that photovoltaic devices based on diblock copolymers had excellent thermal stability owing to the thermally stable film morphology. In this report, it is further demonstrated that block length can be precisely controlled owing to the quasi-living nature of the polymerization. The structures of the copolymers were fully characterized by NMR, UV−vis absorption, fluorescence spectra, and GPC. The film morphology was observed by AFM, and the polymer crystallinity was evaluated by XRD and DSC. Finally, these copolymers were applied to single-component photovoltaic devices, and their charge separation and transport abilities were compared with that of corresponding mixed bulk heterojunction devices.

RESULTS AND DISCUSSION

Synthesis. *Synthesis of Diblock and Random Copolymers with Functional Side Chains.* Scheme 1 shows the synthesis of the monomers and fullerene derivatives. 3-Hexylthiophene (**1**) and 3-(6-bromohexylthiophene) (**4**) were selectively brominated at the 2-position and subsequently iodated at the 5-

dx.doi.org/10.1021/ma300376m | Macromolecules 2012, 45, 6424−6437

Scheme 2. Synthetic Routes for Fullerene-Attached Diblock (D_1, D_2, and D_3) and Random (D_R) Copolymers[a]

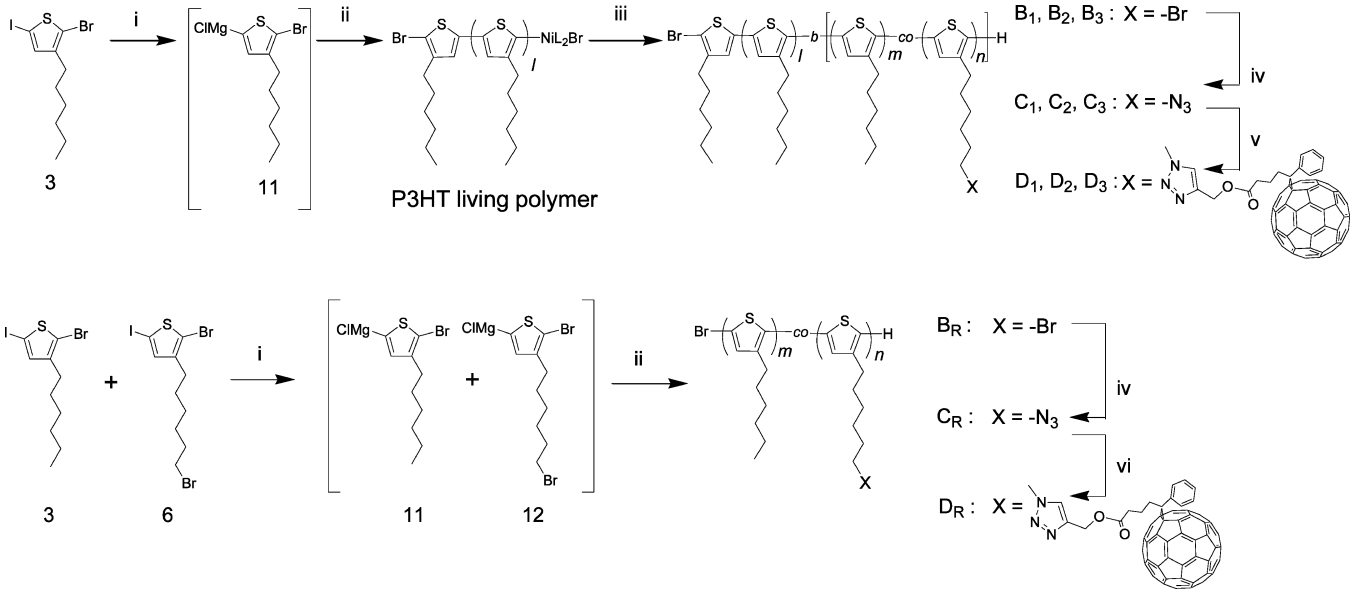

[a]Reagents and conditions: (i) THF, *i*-Pr-MgCl, 0 °C; (ii) Ni(dppp)Cl_2, 35 °C; (iii) **11** + **12** or **12**, 35 °C; (iv) toluene/H_2O, NaN_3, *n*-Bu_4NBr, reflux; (v) **10**, CuBr, PMDETA, *o*-xylene, 50 °C; (vi) **10**, CuBr, PMDETA, *o*-xylene, rt.

Table 1. Summary of the Monomer Ratios and Molecular Weights of Hexylbromide-Functionalized Diblock (B_1−B_3) and Random Copolymers (B_R)

	monomer feed ratios *l*:*m*:*n*	M_n (M_w/M_n)[a] first block	M_n (M_w/M_n)[a] total	calcd ratios of the blocks[b] *l*:(*m* + *n*)	ratio of −Br group[c] (*l* + *m*):*n*
B_1	72:14:14	19 500 (1.06)	24 300 (1.09)	80:20	89:11
B_2	79:7:14	21 300 (1.09)	25 000 (1.10)	85:15	89:11
B_3	83:0:17	21 200 (1.11)	23 700 (1.15)	89:11	89:11
B_R	0:89:11		22 600 (1.11)		89:11

[a]Measured by GPC. [b]Calculated by dividing M_n by the molecular weight of the monomer units. [c]Calculated from the $-CH_2-$ peak intensity in ^1H NMR.

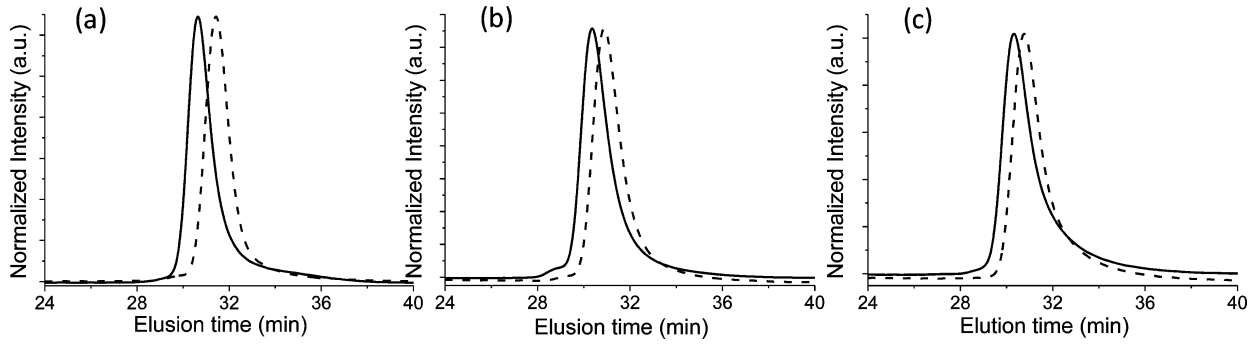

Figure 1. GPC traces of bromide-functionalized diblock copolymers (a) B_1, (b) B_2, and (c) B_3. The broken and solid lines are for P3HTs in the first step and diblock copolymers in the second step, respectively.

position to obtain monomers **3** and **6**, respectively. The fullerene derivative with alkyne functionality (**10**) was synthesized in a high yield from commercially available PCBM (**7**) by following the report.[31,32] The poly(3-alkylthiophene)-based diblock copolymer was synthesized as shown in Scheme 2. Polymer synthesis relies on the controlled synthesis of regioregular poly(3-alkylthiophene)s by the GRIM method and quasi-living polymerization with Ni(dppp)Cl_2 as the catalyst, based on the reports by McCullough et al. and Yokozawa et al.[33,34] It was previously demonstrated that poly(3-hexylthiophene-*b*-3-(2-ethylhexyl)thiophene)s with well-defined structures can be synthesized by optimizing the reaction conditions, and this synthesis was extended to diblock copolymers with functionalized side chains.[35−39] In the first step, the GRIM product of 2-bromo-5-iodo-3-hexylthiophene (**3**) was polymerized with the Ni catalyst to obtain the P3HT living polymer. A mixture of the GRIM products of 2-bromo-5-iodo-3-(6-bromohexyl)thiophene (**6**) and **3** or only the GRIM product of **6** was subsequently added to the living polymer solution to extend the polymer chain by the chain-growth

dx.doi.org/10.1021/ma300376m | *Macromolecules* 2012, 45, 6424−6437

Table 2. Summary of the Monomer Ratios and Molecular Weights of Azide-Functionalized Diblock (C_1–C_3) and Random Copolymers (C_R) and the Monomer Ratios and Fullerene Contents of Fullerene-Functionalized Diblock (D_1–D_3) and Random Copolymers (D_R)

					ratio of fullerene group[b]	
	M_n (M_w/M_n)[a]	ratio of $-N_3$ group[b] $(l + m):n$		M_n (M_w/M_n)[c]	$(l + m):n$	calcd fullerene derivative (**10**) content (wt %)
C_1	23400 (1.10)	89:11	D_1	24300 (1.37)	89:11	38
C_2	24300 (1.15)	89:11	D_2	25600 (1.35)	89:11	38
C_3	22800 (1.17)	89:11	D_3	23300 (1.28)	89:11	38
C_R	21800 (1.12)	89:11	D_R	21400 (1.18)	89:11	38

[a]Measured by GPC. [b]Calculated from the $-CH_2-$ peak intensity in ^1H NMR. [c]Measured by GPC. It is noted that GPC charts of fullerene attached copolymers show unusual behavior.

Scheme 3. Model Fullerene Azide–Alkyene Click Chemistry Reaction

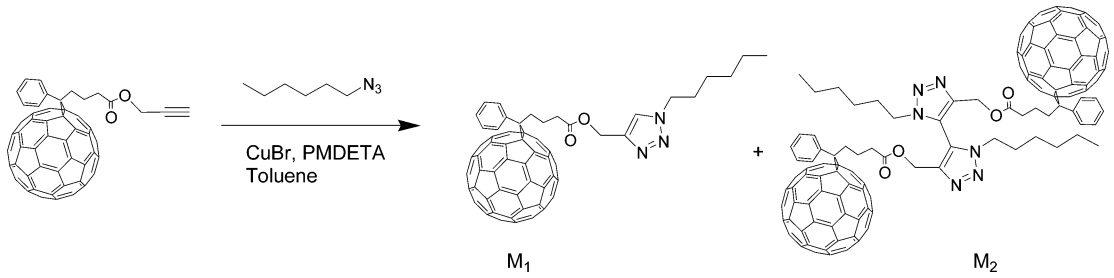

mechanism to form the block copolymer. The domain length of the first P3HT block (l in Scheme 2) and second block ($m + n$) were systematically controlled by changing the monomer feed ratios while keeping the (6-bromohexyl)thiophene contents (n) of the polymers constant (see Table 1).

The GPC charts of the three polymers in the first and second steps are shown in Figure 1. The peak shifted to a higher molecular weight while maintaining the unimodal shape before and after the addition of the second monomers, indicating successful diblock copolymer synthesis. Furthermore, the GPC analysis confirmed that the relative length of the first P3HT block and the second block could be controlled by changing the monomer feed ratios. The molecular weights and polydispersity in the first and second step are summarized in Table 1. A random copolymer with an alkyl bromide side chain was also synthesized as a control using a mixture of monomers **3** and **6** (Scheme 2). Since **3** and **6** have similar structures, the reactivity ratios in the copolymerization are expected to be similar between the monomers. To confirm this, the monomer consumption rates of **11** and **12** were monitored during the synthesis of the copolymer with the feed ratio of 1:1. The relative monomer concentration was determined by GC-MS in the presence of naphthalene as an internal standard following the reported procedure.[33] The time course of the consumption in Figure S1 (Supporting Information) clearly show that the monomers **11** and **12** were consumed in a similar rate during the polymerization, indicating the similar reactivity ratios and the formation of the random copolymer. The GPC analysis of all these diblock and random copolymers show that the number-averaged molecular weight (M_n) was more than 20 000 with a narrow polydispersity (M_w/M_n) of around 1.1. Furthermore, the ratio of 3-hexyl and 3-(6-bromohexyl) side chains observed via ^1H NMR was 89:11 in all the copolymers (Table 1). This ratio is consistent with the feed ratio in the case of the random copolymer but slightly different in the case of the diblock copolymers.

After the polymers were purified by washing with 5 M HCl solution[40] and Soxhlet extraction, bromide groups in the side chain of the diblock and random copolymers were converted to azide groups by reaction with NaN_3 in water/toluene in the presence of n-Bu_4NBr as a phase transfer catalyst (Scheme 2). All the bromide groups were quantitatively converted into azide groups without any side reactions (Table 2), which was confirmed by the complete disappearance of the methylene proton peaks next to bromine at 3.42 ppm and the appearance of the methylene proton peaks next to azide at 3.28 ppm in the ^1H NMR spectra (see Figures S5 and S6 in Supporting Information). Substitution reaction between NaN_3 and the bromide group at the 2-position of the thiophene at the chain end is not likely considering the reactivity of aromatic halides. This is supported by a model reaction between **5** and NaN_3 in the similar conditions in which only the bromide groups at the alkyl side chain were completely converted into azide groups but there was no reaction at the 2-position (Scheme S1 and Figure S2 in Supporting Information).

Investigation of Fullerene Azide–Alkyne Click Chemistry and Synthesis of Fullerene-Attached Copolymers. To apply for the polymer/fullerene connecting reaction, it is very important that the click reaction proceeds in high yield with high selectivity, since side reactions could lead to lowering of the conversion and polymer cross-linking. On the basis of the observations, two points will be addressed here for achieving quantitative attachment of the fullerene to the copolymers. First, the click reaction needed to be conducted in the absence of oxygen in a proper solvent; otherwise, a large insoluble fraction would have formed during the reaction. To clarify the reason for this, a model reaction between **10** and hexyl azide was performed using the same catalysts (Scheme 3). When this reaction was performed in air, in addition to the formation of $\mathbf{M_1}$ as the major product, the bis-triazole fullerene dimer $\mathbf{M_2}$, as a byproduct, was observed with 4%–13% yield from the ^1H NMR and mass spectra (see Figures S9 and S10 in the Supporting Information and Experimental Section for details).

dx.doi.org/10.1021/ma300376m | *Macromolecules* 2012, 45, 6424–6437

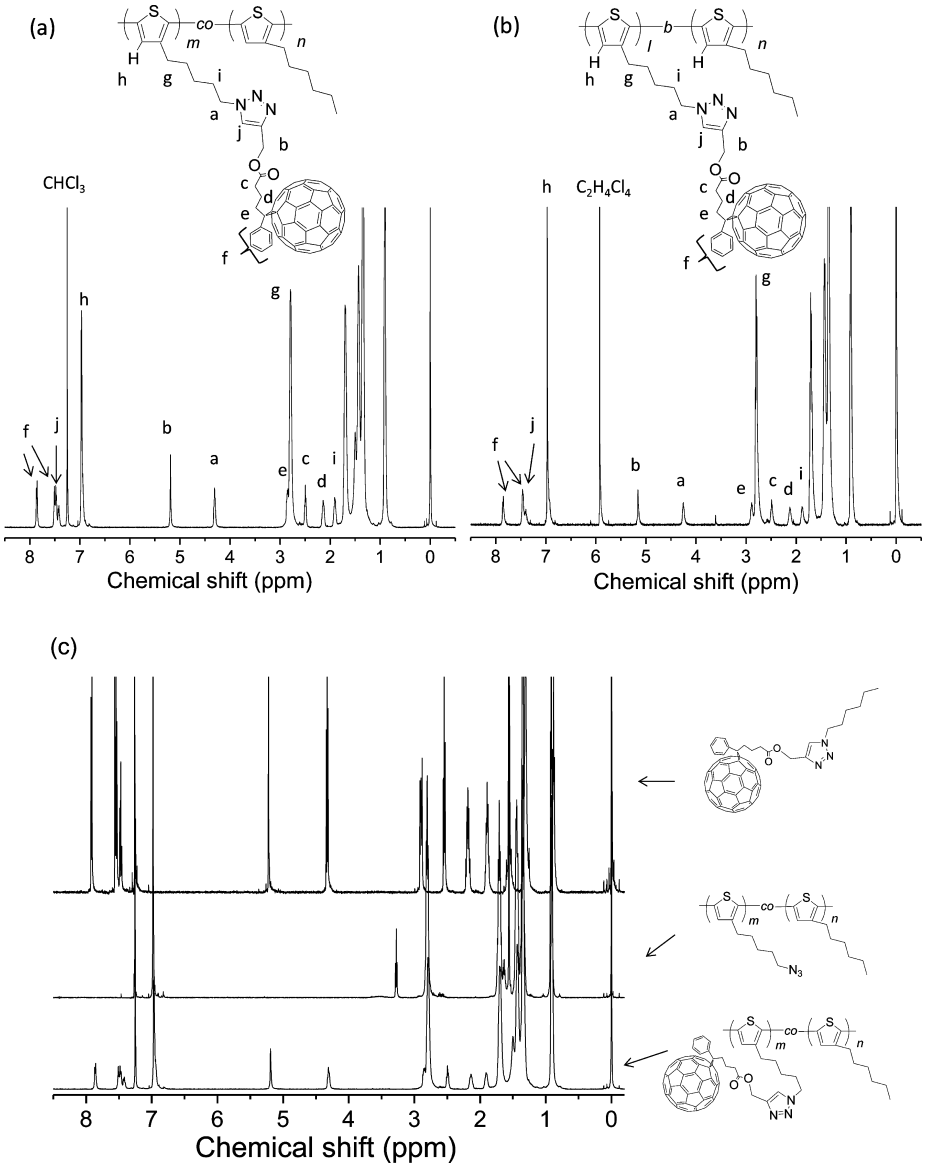

Figure 2. ^{1}H NMR spectra of fullerene-attached (a) random copolymer $\mathbf{D_R}$ in $CDCl_3$, (b) diblock copolymer $\mathbf{D_3}$ in $C_2D_2Cl_4$ (100 °C), and (c) random copolymer $\mathbf{C_R}$, the fullerene model compound $\mathbf{M_1}$, and $\mathbf{D_R}$ in $CDCl_3$.

The formation of the bis-triazole compound during the Cu(I)-catalyzed azide−alkyne reaction in oxidative conditions was mentioned by Sharpless et al. and recently investigated in detail by Burgess et al.[28,41] Furthermore, the model reaction under air also sometimes produced unknown insoluble materials. The removal of oxygen and oxidative impurities in the amine for the Cu(I) ligand prevented these unfavorable side reactions and also led to the complete conversion of the starting material in the model reaction. Note that side product derived from thermally induced cycloaddition reaction between the azide group and C_{60} core was not observed in ^{1}H NMR and ^{13}C NMR spectra in this model reaction at 50 °C[25,42] (see Experimental Section and Figure S11).

The second important point of this reaction is the addition of excess amounts of **10** per azide group of the polymer side chain (typically 2−4 equiv). A fraction with higher molecular weight was observed in the GPC charts when the amount of **10** was small, which could be attributed to the loosely cross-linked polymers (Figure S12). The formation of the insoluble fraction was more significant when the azide density in the copolymer was high (the local densities of the azide are in the order of $\mathbf{D_3} > \mathbf{D_2} > \mathbf{D_1} > \mathbf{D_R}$). However, this fraction did not form when an excess of **10** per azide side chain was used, as confirmed by GPC. It should be emphasized again that controlling the reaction conditions is critically important; otherwise, further characterization or the application to photovoltaic cells becomes difficult owing to the limited polymer solubility. The completely soluble fullerene-attached random ($\mathbf{D_R}$) and diblock copolymers ($\mathbf{D_1}$−$\mathbf{D_3}$) synthesized under optimized reaction conditions were subjected to the following characterizations.

Characterization of Fullerene-Attached Copolymers. *Polymer Solubility, ^{1}H NMR and FT-IR Spectra.* The fullerene-attached random copolymer ($\mathbf{D_R}$) has a good solubility of more than 30 g L^{-1} in $CHCl_3$ or chlorobenzene at room temperature. The fullerene-attached diblock copolymers ($\mathbf{D_1}$−$\mathbf{D_3}$) are also soluble in the solvents at slightly higher temperatures (more than 30 g L^{-1} in chlorobenzene at 40 °C). There was no observable difference in the solubility of the diblock copolymers

dx.doi.org/10.1021/ma300376m | *Macromolecules* 2012, 45, 6424−6437

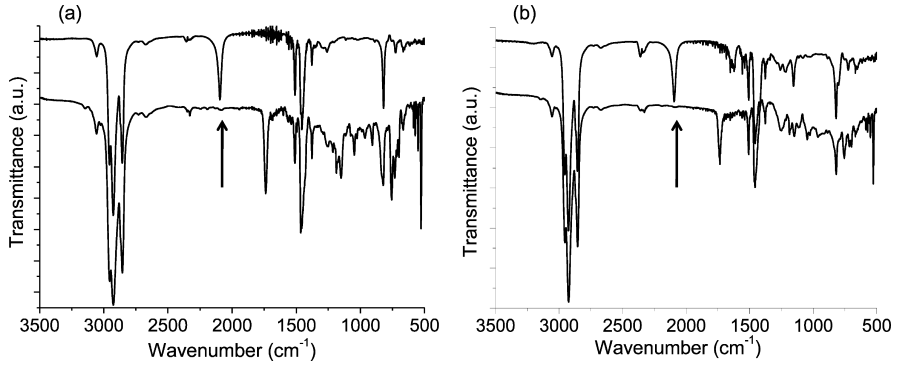

Figure 3. FT-IR spectra of (a) random copolymers $\mathbf{C_R}$ (top) and $\mathbf{D_R}$ (bottom) and (b) diblock copolymers $\mathbf{C_3}$ (top) and $\mathbf{D_3}$ (bottom). Arrows indicate the disappearance of the azide vibration peaks.

$\mathbf{D_1}$–$\mathbf{D_3}$, although the fullerenes are quite densely attached at the side chain of the second block in $\mathbf{D_3}$.

Figures 2a and 2b show the ^{1}H NMR spectra of $\mathbf{D_R}$ and $\mathbf{D_3}$, respectively, with the peak assignments of the protons belonging to the fullerene-attached units. In Figure 2c, the ^{1}H NMR spectrum of $\mathbf{D_R}$ is compared to that of the azide-functionalized precursor polymer $\mathbf{C_R}$ and the model fullerene compound $\mathbf{M_1}$ to explain the progress of the click reaction. The data show that all azide groups in the precursor polymer were reacted with alkyne, as confirmed by the complete disappearance of the peaks at 3.28 ppm, which could be assigned to the methylene protons next to the azide. The new peaks that appeared at around 5.19 and 4.31 ppm after the reaction were assigned to the methylene protons next to the triazole ring,[43] which is clear evidence of the covalent attachment between the fullerene derivative and the polymers. The peak signal integration analysis agrees with the complete conversion from the azide group to the triazole ring in the side chain of the polymers (11 mol % of the thiophene units). These assignments and claims are also the same in the diblock copolymers $\mathbf{D_3}$ (Figure 2b), $\mathbf{D_1}$, and $\mathbf{D_2}$ (Figure S7). The fullerene derivative (**10**) contents of random copolymer $\mathbf{D_R}$ and diblock copolymers $\mathbf{D_1}$–$\mathbf{D_3}$ are all around 11 mol % of the thiophene unit, corresponding to 38 wt % of the copolymers in this analysis (Table 2). The FT-IR spectra of the random and diblock copolymers before and after the click reaction also showed that the peak derived from the azide group at around 2100 cm^{-1} completely disappeared after the reaction (Figure 3 and Figure S15).

UV–vis Absorption and Fluorescence Spectra. UV–vis absorption spectra of the fullerene-attached copolymers in solution are shown in Figure 4. The spectrum of the P3HT:PCBM physical mixture (1.0:0.6 by weight ratio) is also presented for comparison. Both the peak maxima and the relative intensities of the fullerene-attached polymers are similar to those of the mixtures, suggesting little intra- or intermolecular aggregation in the copolymers. Fullerene absorption bands appeared at 260 and 330 nm. The fullerene contents introduced into the copolymers can be estimated by a comparison of these absorption intensities at 260 nm to those of the physical mixture. This is possible because the unreacted fullerene is uncontaminated, as shown by the GPC analysis in the following section. The fullerene derivative (**10**) content estimated in this analysis is 37 wt % for $\mathbf{D_R}$ and 35 wt % for $\mathbf{D_3}$, which is fairly close to the ^{1}H NMR estimate. This result further supports the theory that the fullerene derivatives were quantitatively attached to the polymer side chain. The slightly

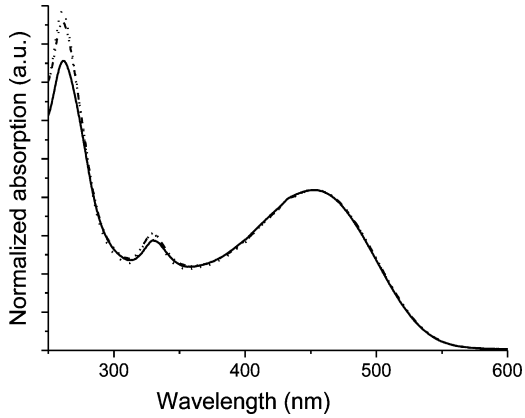

Figure 4. Absorption spectra of P3HT:PCBM physical mixture (1.0:0.6 by weight) (solid) and fullerene-attached random $\mathbf{D_R}$ (dashed) and diblock $\mathbf{D_3}$ (dotted) copolymers in $CHCl_3$ solution. The spectra are normalized at 450 nm.

lower peak intensity at 260 nm in block $\mathbf{D_3}$ (Figure 4), compared to the others, might be explained by fullerene absorption broadening, which could have arose from the weak intramolecular interactions between the fullerene derivatives because they are quite densely attached in $\mathbf{D_3}$. This fullerene ratio in the copolymers corresponds to the weight ratio of 1.0:0.6 for P3HT:PCBM, which is close to the optimum ratio of photovoltaic devices with the mixed bulk heterojunction of P3HT:PCBM.

Fluorescent spectra of the fullerene-attached polymers in solution are investigated. The fluorescence from P3HT is not quenched by blending PCBM in the solution (Figure 5) because intermolecular electron or energy transfers from P3HT to PCBM can be neglected in the diluted solutions (the absorbance of P3HT is around 0.2). However, the fullerene-attached copolymers showed significant P3HT fluorescence quenching owing to the close proximity of P3HT and the fullerene covalent attached to the polymer side chains. The quenching efficiency in the diblock copolymer $\mathbf{D_3}$ is much lower (about 40% was quenched) than that of the random copolymer $\mathbf{D_R}$ (about 90% was quenched), despite having similar amounts of fullerene. This difference could reflect the difference in the fullerene position in the copolymers. The electron or energy transfer from P3HT to the fullerenes could be efficient in all $\mathbf{D_R}$ polymer chains in which the fullerenes are uniformly distributed. In contrast, the diblock copolymers have pure P3HT blocks in which the diffusing excited states could not find fullerenes and emit fluorescence during their lifetimes.

dx.doi.org/10.1021/ma300376m | *Macromolecules* 2012, 45, 6424–6437

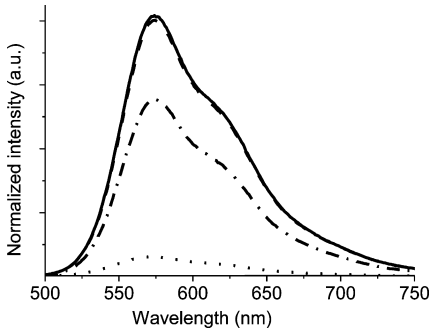

Figure 5. Fluorescent spectra in $CHCl_3$ solution of P3HT (solid), P3HT:PCBM physical mixture (1.0:0.6 by weight) (dashed), fullerene attached diblock $\mathbf{D_3}$ (solid dotted), and random $\mathbf{D_R}$ (dotted) copolymers. Excitation wavelength: 450 nm.

We concluded that these quenching behaviors are qualitatively consistent with the structural difference between $\mathbf{D_R}$ and $\mathbf{D_3}$.

Gel Permeation Chromatography (GPC) Analysis. GPC traces of the fullerene-attached copolymers with detection wavelengths of 260 or 500 nm are shown in Figure 6. The former wavelength can be mainly attributed to fullerene absorption and the latter to polythiophene absorption. There are two peaks in GPC charts before purification of the polymers (trace iii). Each peak was collected and analyzed by UV−vis absorption spectra, which confirmed that the one at around 30 min is the fullerene-attached copolymers and the one at 43 min is unreacted PCBP (**10**) (Figure S14). After purification by reprecipitation into CH_2Cl_2 or directly separating two fractions by using preparative GPC, the peak at 43 min completely disappeared. Considering the high absorption coefficient of **10** at 260 nm, contamination of the fullerene derivative in the copolymer can be excluded. When the detection wavelengths of 260 and 500 nm were used for the copolymers (traces i and ii), the two traces almost matched, indicating that the fullerenes are uniformly attached to the polymers, independent of the molecular weight. The small shoulder of the polymer peaks at the side of the shorter elution time might be due to the aggregation or slight cross-linking of the polymers.

The quantitative attachment of the fullerene derivative should increase the molecular weight of the copolymers by ca. 15 000, calculated from the unit ratios and the molecular weight of fullerene. Therefore, it is unexpected that the GPC charts of both the fullerene-attached random ($\mathbf{D_R}$) and diblock copolymers ($\mathbf{D_3}$) did not shift compared to the precursor azide-functionalized polymers ($\mathbf{C_R}$ and $\mathbf{C_3}$), as shown in Figure 6 (traces i and iv). Since all the other data support fullerene attachment at the side chains, this unexpected behavior in the GPC might be attributed to the conformational change in the polymers in the $CHCl_3$ solution after fullerene attachment, owing to the intramolecular interactions between the fullerene groups and between the polythiophene and fullerene, resulting in the reduction of the effective polymer volume. Similar GPC behavior was observed in fullerene-attached polystyrene,[44] and other polymers[26,45] showed even lower effective volumes after acceptor group attachment. Another possibility is that triazole functionality or fullerenes could change the affinity between the polymer and the polystyrene-based GPC column.

UV−vis Absorption Spectra in Films. Although the polymers $\mathbf{D_3}$ and $\mathbf{D_R}$ did not show absorption spectra differences in the solution, they showed remarkable differences in the absorption of the films (Figure 7). The diblock copolymer $\mathbf{D_3}$ film shows a polythiophene absorption red-shift compared to that in the solution, with an intense shoulder around 600 nm, which indicates the existence of the crystalline domain in the polymer.[46] This change is similar to that observed in the mixture of P3HT and PCBM films. In contrast,

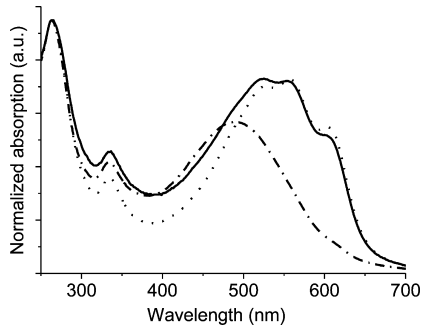

Figure 7. UV−vis absorption spectra of as-casted films of P3HT:PCBM physical mixture (1.0:0.6 by weight) (dotted), fullerene-attached random $\mathbf{D_R}$ (solid dotted), and diblock $\mathbf{D_3}$ (solid) copolymers. The spectra are normalized at 260 nm.

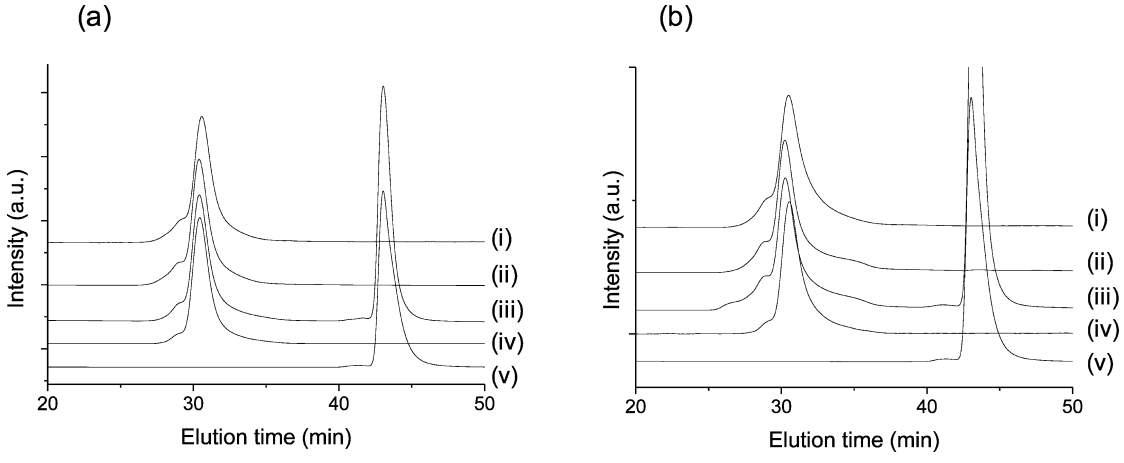

Figure 6. GPC traces of (a) random and (b) diblock copolymers. GPC trace of the fullerene-attached polymers ($\mathbf{D_R}$ and $\mathbf{D_3}$) with detection wavelengths of (i) 500 nm, (ii) 260 nm, (iii) fullerene-attached polymers ($\mathbf{D_R}$ and $\mathbf{D_3}$) before purification, (iv) azide-functionalized polymers ($\mathbf{C_R}$ and $\mathbf{C_3}$), and (v) PCBP (**10**).

dx.doi.org/10.1021/ma300376m | *Macromolecules* 2012, 45, 6424−6437

the random copolymer $\mathbf{D_R}$ film showed only a slight peak red-shift in comparison to the solution and showed quite low absorption shoulder. This result indicates that fullerene attachment at the side chains decreases the crystallinity of the polythiophene backbones in the films, probably because of the bulky nature of the fullerene. The crystallinity of P3HT was therefore lost in $\mathbf{D_R}$ because the fullerenes were uniformly attached to entire polymer chains. In contrast, the P3HT blocks in $\mathbf{D_3}$ maintained high crystallinity, similar to the P3HT homopolymer blended with PCBM, because the blocks were physically separated from the fullerene-attached blocks.

Differential Scanning Calorimetry (DSC) Analysis. The existence of the crystalline domain in the diblock copolymer $\mathbf{D_3}$ is also supported by differential scanning calorimetry (DSC) analysis. The first cycle DSC chart of $\mathbf{D_3}$ showed both a melting peak at 223 °C and a recrystallization peak at 130 °C, similar to the P3HT homopolymer (Figure S17). In contrast, the random copolymer $\mathbf{D_R}$ showed no detectable peaks. It was found that these fullerene-attached copolymers start cross-linking above 200 °C, the DSC peaks of $\mathbf{D_3}$ become smaller after the second cycle, and the peak temperature shifts to lower temperatures. This behavior is similar to that previously reported for the thermally cross-linkable polymer;[37] this behavior makes it difficult to further quantitatively analyze the crystallinity of the polymer. This polymer cross-linking could be due to triazole functionality decomposition.[47]

X-ray Diffraction (XRD) Analysis of Thin Films. The crystalline structure of the copolymer thin films was investigated by X-ray diffraction (XRD) (Figure 8). The

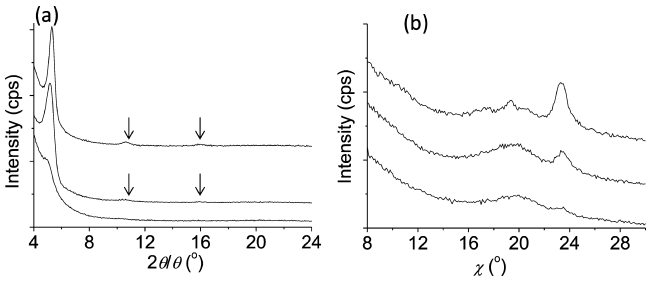

Figure 8. (a) Out-of-plane and (b) in-plane X-ray diffraction patterns of the annealed films of P3HT:PCBM physical mixture (1.0:0.6 by weight) (top), fullerene-attached diblock $\mathbf{D_3}$ (middle), and random $\mathbf{D_R}$ (bottom) copolymers.

P3HT:PCBM physical mixture and the fullerene-attached diblock copolymer films showed diffraction peaks at low angles in the out-of-plane measurements, attributable to a lamellar structure typically observed in crystalline regioregular P3HT. The *d*-spacings of the diffraction from (100), (200), and (300) are 16.6, 8.33, and 5.54 Å, respectively, for the P3HT:PCBM physical mixture and 17.1, 8.42, and 5.57 Å, respectively, for the diblock copolymer $\mathbf{D_3}$. A peak was also observed in the in-plane diffraction at 3.82 Å for both the physical mixture of P3HT and PCBM and $\mathbf{D_3}$, corresponding to the $\pi-\pi$ stacking distance between the polythiophene chains (Figure 8). These results indicate that the diblock copolymer $\mathbf{D_3}$ has similar lamellar and $\pi-\pi$ stacking crystalline structures to P3HT, although its lamellar distance is slightly longer. In contrast, the film of the random copolymer $\mathbf{D_R}$ showed a small peak from (100) in the out-of-plane diffraction pattern, and a broad and weak peak was observed at 3.82 Å in the in-plane diffraction. This result indicates that the random attachment of fullerenes largely disturbed the crystalline packing of the copolymer $\mathbf{D_R}$. This coincides with the conclusion from the difference in UV−vis absorption spectra in the films discussed above.

Morphological Investigation by Atomic Force Microscopy (AFM). The nanostructures of fullerene-attached polymer films were investigated using tapping mode AFM height and phase images (Figure 9). The polymer films were annealed at 150 °C for 60 min before the measurements. All the height images show flat surfaces with R_a of around 1 nm in which the nanopatterns are not quite clear. In the phase images, the fullerene-attached diblock copolymers $\mathbf{D_1}-\mathbf{D_3}$ showed clear nanopatterns. $\mathbf{D_1}$ and $\mathbf{D_2}$ films show similar fibrous structures with widths of ca. 20 nm, whereas the $\mathbf{D_3}$ film looks more spherical with a width of ca. 20 nm. This is in contrast to the random copolymer $\mathbf{D_R}$, which just showed a featureless image. It is important to mention that similar $\mathbf{D_3}$ structures were observed in real photovoltaic devices, with thicknesses of about 90 nm after thermal annealing. The nanopattern formations could be attributed to the separation of the crystalline P3HT block and the fullerene-attached blocks, and the differences in patterns between $\mathbf{D_1}-\mathbf{D_2}$ and $\mathbf{D_3}$ could reflect the differences in the block ratios.

In contrast to coil−coil type diblock copolymers, in which microphase-separated structures such as lamella, gyroid, cylinder, and sphere are finely tuned by the volume fraction of each block, the morphological behavior of rod−coil or rod−rod type block copolymers is complicated and largely affected by crystallization of the segment.[48] As observed for several block copolymers, P3HT domains tend to self-assemble into fibril-like structures by crystallization and separate themselves from the other blocks.[21,48−52] In $\mathbf{D_1}-\mathbf{D_3}$ films, the fullerene-attached domains could aggregate to surround this P3HT fibrous domain. However, the relatively high fullerene volume and density in the second block could disturb this P3HT fibrous structure. In fact, the out-of-plane XRD pattern of the $\mathbf{D_1}-\mathbf{D_3}$ thin film showed that the lamellar distance of the P3HT crystalline structure is slightly longer than that of pure P3HT (Figure 8 and Figure S16). This structural disturbance could build up as the crystalline P3HT fibril grows, and therefore, it could make the persistent length of the fibril in $\mathbf{D_1}$ and $\mathbf{D_2}$ shorter than the other rod−rod or rod−coil type P3HT block copolymers.[35,51] The attachment of the highest density fullerene in $\mathbf{D_3}$ could significantly disturb the fibril formation, and the structure might appear more spherical in the AFM phase image.

Photovoltaic Device Performance. Photovoltaic devices were fabricated with the fullerene-attached diblock copolymers $\mathbf{D_1}-\mathbf{D_3}$ to investigate the effects of the block lengths. Device performances were first optimized by changing the film thicknesses, and the best results are compared in Table 3. J_{SC} was improved from 5.19 to 7.04 mA cm^{-2} on increasing the length of the first P3HT block and reducing the length of the second block from $\mathbf{D_1}$ to $\mathbf{D_3}$, but V_{OC} was slightly lowered from 0.54 to 0.50 V. FF remained almost constant at around 0.6, and the optimum film thickness increased from 56 to 85 nm from $\mathbf{D_1}$ to $\mathbf{D_3}$. The higher J_{SC} and the larger optimum film thickness could be explained by the enhanced polythiophene crystallinity resulting from an increase in the relative ratio of pure P3HT domain in the copolymer or improved acceptor connectivity by densely grafted fullerenes.

Next, the effect of thermal treatment on the photovoltaic performance of the device based on $\mathbf{D_3}$ was investigated. As shown in Table 4, the diblock copolymer showed much better

dx.doi.org/10.1021/ma300376m | *Macromolecules* 2012, 45, 6424−6437

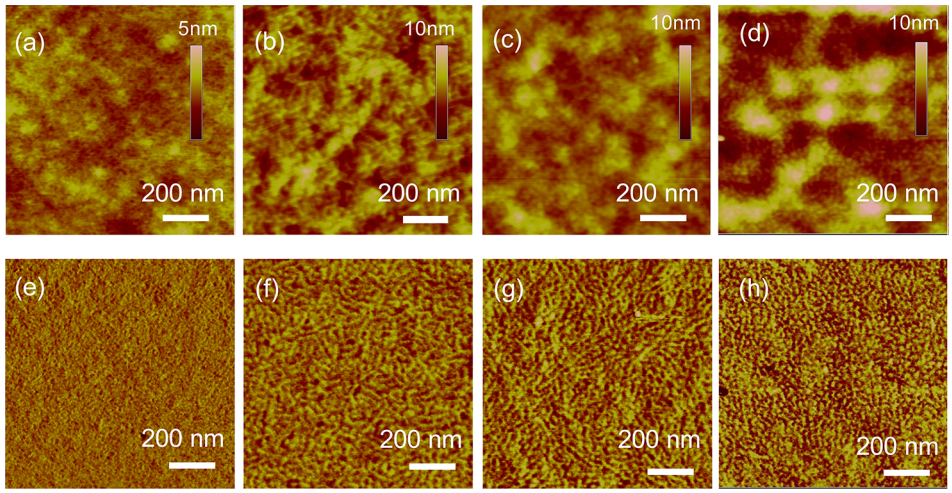

Figure 9. AFM height (a–d) and phase images (e–h) of annealed copolymer films: (a, e) $\mathbf{D_R}$, (b, f) $\mathbf{D_1}$, (c, g) $\mathbf{D_2}$, and (d, h) $\mathbf{D_3}$.

Table 3. Effect of Block Ratio in the Fullerene-Attached Diblock Copolymers on Device Properties[a]

polymer	J_{SC} (mA/cm^2)	V_{OC} (V)	FF	PCE (%)	optimum film thickness (nm)
$\mathbf{D_1}$	5.19	0.54	0.59	1.64	56 ∓ 3
$\mathbf{D_2}$	6.74	0.51	0.57	1.94	75 ∓ 4
$\mathbf{D_3}$	7.04	0.50	0.60	2.13	85 ∓ 3

[a]Spin-coated from mixed solvent (chlorobenzene:$CHCl_3$ = 3:2). Post-thermal annealing at 140 °C for 30 min.

Table 4. Effect of Annealing Conditions on the Device Properties of $\mathbf{D_3}$

condition	J_{SC} (mA/cm^2)	V_{OC} (V)	FF	PCE (%)
as-cast	4.04	0.48	0.50	0.97
140 °C, 30 min	7.04	0.50	0.60	2.13
180 °C, 90 min	7.61	0.50	0.62	2.34

performance after thermal annealing. The optimum annealing temperature and time for $\mathbf{D_3}$ were 180 °C for 90 min. This represents a much higher temperature and longer time than that for the P3HT:PCBM physical mixture; this condition generally causes severe phase separation and the formation of large PCBM crystals.[53] The high long-term thermal stability of the fullerene-attached diblock copolymers was demonstrated in our previous report.[27] It is worth noting that performance of the device based on the random copolymer $\mathbf{D_R}$ was not sensitive to the annealing conditions. In addition, the introduction of buffer layers like LiF improved the performance in the $\mathbf{D_R}$ devices but did not affect the performances of the block copolymers.

The best device performances of the copolymers after the optimization of the fabrication conditions are summarized in Table 5 along with the performance of the P3HT:PCBM bulk heterojunction device. *J*–*V* curves of the devices under the simulated solar light irradiation are shown in Figure 10. The device with the diblock copolymers $\mathbf{D_3}$ showed a much higher device performance than the random copolymer $\mathbf{D_R}$. The 2.46% power conversion efficiency (PCE) of the diblock copolymer $\mathbf{D_3}$ is the highest value in photovoltaic cells consisting of a single component (i.e., no mixing of the donor and acceptor materials). The high V_{OC}, low J_{SC}, and low FF of the random copolymer $\mathbf{D_R}$ can be explained by the

Table 5. Optimized Device Performance of the Fullerene-Attached Random ($\mathbf{D_R}$) and Diblock ($\mathbf{D_3}$) Copolymers and the Physical Mixture

polymer	J_{SC}(mA/cm^2)	V_{OC} (V)	FF	PCE (%)
D_R[a]	1.76	0.76	0.33	0.45
D_3[b]	8.14	0.48	0.63	2.46
P3HT/PCBM[c]	8.61	0.54	0.66	3.07

[a]As-cast film with LiF buffer layer. [b]Post-thermal annealing at 180 °C for 90 min. Using chloronaphthalene as an additive for spin-coating. [c]P3HT:PCBM = 1.0:0.6 wt %. Post-thermal annealing at 140 °C for 30 min.

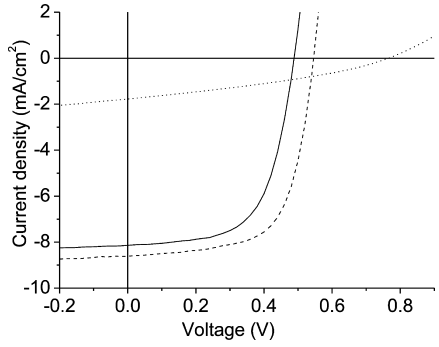

Figure 10. *J*–*V* curves of the photovoltaic devices with P3HT:PCBM physical mixture (dashed), fullerene-attached random $\mathbf{D_R}$ (dotted), and diblock $\mathbf{D_3}$ (solid) copolymers under simulated solar light irradiation (AM1.5).

amorphous nature of this polymer; it was reported that the bulk heterojunction of less crystalline regiorandom P3HT and PCBM shows a much higher V_{OC} and lower J_{SC} than crystalline regioregular P3HT because of the larger band gap and therefore deeper energy level of the highest occupied molecular orbital (HOMO).[54] The UV–vis, XRD, and DSC data shown above indicate that the random copolymer $\mathbf{D_R}$ has low crystallinity owing to the random attachment of the bulky fullerenes.

External quantum efficiency (EQE) and the absorption of the optimized devices are compared in Figure 11. Maximum EQE in the diblock copolymer $\mathbf{D_3}$ reached 56% at 510 nm, which is reasonably high when the fact that the film thickness of the optimized device is around 90 nm and the absorbance in the transmittance mode is 0.43 (corresponding to an absorptivity of

dx.doi.org/10.1021/ma300376m | *Macromolecules* 2012, 45, 6424–6437

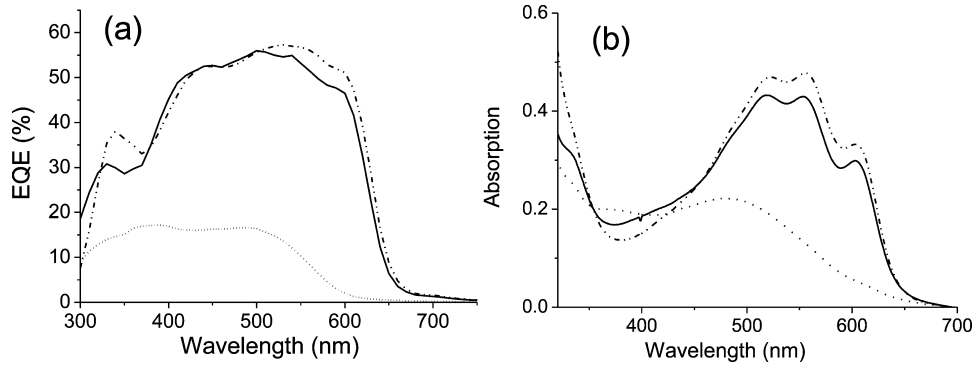

Figure 11. (a) EQE spectra and (b) absorption spectra of the photovoltaic devices of P3HT:PCBM physical mixture (dashed/dotted), fullerene-attached random $\mathbf{D_R}$ (dotted), and diblock $\mathbf{D_3}$ (solid) copolymers.

63% in the transmittance mode) are taken into account (Figure 11b). This EQE value and device thickness are almost comparable to that of the P3HT:PCBM physical mixture (maximum EQE of 57% at 530 nm and absorptivity of 67% in the transmittance mode).

DISCUSSION

In this section, the differences in performance between the devices based on the diblock copolymer $\mathbf{D_3}$ and the corresponding mixed bulk heterojunction (P3HT:PCBM) are discussed. First, although J_{SC} of the $\mathbf{D_3}$ device is slightly lower than that of P3HT:PCBM, the maximum EQE values for both devices are similarly high (56−57%). Accurate estimation of the internal quantum efficiency (IQE) may be difficult because of the interference effects of incident light in the thin films. However, considering that the absorption of the $\mathbf{D_3}$ device is slightly lower than that of P3HT:PCBM in the 500−600 nm range (Figure 11b), the comparable EQE in this region suggests that the charge separation efficiencies are close to each other. The J_{SC} difference under AM1.5 irradiation could be attributable to the different EQE shapes shown in Figure 11a. It should be emphasized here that the grafting ratio of the fullerene of the diblock copolymer $\mathbf{D_3}$ corresponds to P3HT:PCBM = 1.0:0.6 wt %, which is fairly close to the optimum ratio for the P3HT:PCBM system. Considering that all the fullerene groups are attached to the polymer block, this efficient charge separation, comparable to that of the mixed bulk heterojunction, is surprising. The efficiency may be further improved by optimizing the grafting amount of the fullerene. It is also interesting to note that the addition of PCBM to the diblock copolymer $\mathbf{D_3}$ film up to 7 wt % (the resulting ratio corresponds to P3HT:PCBM = 1.0:0.8 wt %) did not change V_{OC}, J_{SC}, FF, and PCE (see Table S2). This result may suggest that the physically mixed domain between P3HT and PCBM might not be necessary for achieving the high J_{SC} observed in the bulk heterojunctions.

The open-circuit voltages of the $\mathbf{D_3}$ devices (~0.49 V) were less, but repeatedly lower than that of the mixture bulk heterojunction of P3HT:PCBM (~0.55 V). Since V_{OC} of the devices is affected by many factors, it is difficult to trace the origin of this difference. The redox potential of the copolymers was analyzed by cyclic voltammetry (CV) in film state. The oxidation potentials of the polymers are summarized in Table S3 and Figure S19 in the Supporting Information. HOMO energy levels of P3HT, the random copolymer ($\mathbf{D_R}$), and the block copolymers are estimated as −5.05, −5.31, and −5.21−5.24 eV, respectively. This energy difference could be explained by the structural disorder of the polythiophenes in the films; P3HT block has an ordered and planar structure resulting in a high-lying HOMO energy levels, while the fullerene-attached block has a disordered and twisted structure and therefore a deeper HOMO level. The block copolymers have the energy values in between since the potentials by CV are averaged over the polymer chains. The higher V_{OC} of 0.76 V was observed in the $\mathbf{D_R}$ device may be explained by deeper HOMO of the polythiophene, in which the hole could only transport in the disordered domain. Recent transient absorption spectroscopy studies suggest that there are two hole transport paths in P3HT:PCBM bulk heterojunction devices:[55] the crystalline and disordered domains of P3HT. Each should have a different energy level, and the recombination kinetics and V_{OC} of the device can be determined by the population ratios of the conducting holes through each path. Since the XRD patterns and AFM images suggest the formation of the crystalline hole transport path of the P3HT block, the nanostructure in the $\mathbf{D_3}$ device might have a larger low-energy hole population in the crystalline path and could result in slightly lower V_{OC}. As for the lowest unoccupied molecular orbital (LUMO) of the acceptor, the reduction potential of the triazole model compound $\mathbf{M_1}$ by CV was virtually the same as PCBM in solution[32] (Figure S18 and Table S1). Therefore, the induction effect of the triazole could be neglected, although the energy level of the fullerene in the film state might still be affected by the intermolecular interaction with these groups. (Reversible reduction peaks of the fullerene groups were not observed by CV in the copolymer films. CV measurements of the copolymer in *o*-dichlorobenzene solution gave broad peaks with very low intensity, and it was difficult to determine the exact reduction potentials.) Another possibility related to the energetics is that the charge transfer (CT) state at the donor/acceptor interface in $\mathbf{D_3}$ could be different from that in the mixed bulk heterojunction.[56] The CT state energy formed at the interface has recently been directly correlated to V_{OC} of the organic photovoltaic devices.[57−59] The difference in the average distance between P3HT and the fullerene group[60] or dipole moment formation[61] might be related to the difference in V_{OC}. Bimolecular recombination, at either the donor/acceptor or organic/inorganic interfaces, might be also responsible, although the insensitivity of V_{OC} to the buffer layer materials described above makes the latter factor less plausible.

The relatively high FF of 0.63 obtained in the $\mathbf{D_3}$ devices indicated that an efficient charge transport pathway is constructed in this single-component system. This FF value is still slightly lower than that of P3HT:PCBM, and the well-

dx.doi.org/10.1021/ma300376m | *Macromolecules* 2012, 45, 6424−6437

optimized bulk heterojunction system sometimes shows high FFs up to ~0.7. Nevertheless, this result in $\mathbf{D_3}$ is quite promising because all the single-component systems reported so far have shown quite low FFs (typically FF of less than 0.4, with several exceptions with FF of 0.46[12,62]), which has been a fundamental limitation to obtaining efficient photovoltaic performance. These results indicated that this single-component system by using self-organization of diblock copolymer could become an alternative rational way to precisely control the morphology of the donor and the acceptor with a high performance.

CONCLUSION

Well-defined fullerene-attached poly(3-alkylthiophene)-based copolymers were synthesized using the GRIM polymerization and azide−alkyne click chemistry. The synthesized diblock copolymers have crystalline structures similar to P3HT and self-assemble to form a nanopattern in the AFM phase image. As a result, the photovoltaic performance of diblock copolymer $\mathbf{D_3}$ showed 2.5% power conversion efficiency with an FF of 0.63. This result demonstrated that single-component donor−acceptor block polymers could become an alternative rational design for the active layer of devices, which currently relies on a physically mixed system. Our system could also be an interesting model system; many analytical methods developed so far for the mixed P3HT:PCBM system could be applicable for elucidating the effect of well-defined nanostructures on the charge generation, transport, and recombination behaviors in photovoltaic devices.

EXPERIMENTAL SECTION

Synthesis. All reagents were used as received from the provider unless otherwise stated. The ^{1}H NMR spectra of the synthesized compounds are shown in the Supporting Information. 3-Hexylthiophene (**1**), 2-bromo-3-hexylhtiophene (**2**), 2-bromo-5-iodohexylthiophene (**3**), and 3-(6-bromohexyl)thiophene (**4**) were synthesized as previously reported.[35−37]

2-Bromo-3-(6-bromohexyl)thiophene (5). 3-(6-Bromohexyl)-thiophene (**4**) (14.0 g, 56.6 mmol) was dissolved into 100 mL of THF in a 200 mL round flask. After cooling the reaction solution at 0 °C, *N*-bromosucciimide (9.68 g, 54.4 mmol) was added, and the reaction mixture was stirred at 0 °C overnight. THF in the reaction mixture was evaporated, and the residue was extracted by hexane after the reaction. The organic layer was sequentially washed with 10% $Na_2S_2O_3$(aq) twice, with 10% KOH(aq) once, and with water twice. The hexane in the solution was evaporated after being dried with $MgSO_4$ and filtered. The residue was purified by vacuum distillation to obtain pure 2-bromo-3-(6-bromohexyl)thiophene (**5**) (14.0 g, 42.9 mmol) in 76% yield. ^{1}H NMR (500 MHz, $CDCl_3$): δ 7.20−7.17 (d, 1H), 6.79−6.76 (d, 1H), 3.40 (t, 2H), 2.57 (t, 2H), 1.86 (m, 2H), 1.59 (m, 2H), 1.45 (m, 2H), 1.35 (m, 2H).

2-Bromo-5-iodo-3-(6-bromohexyl)thiophene (6). 2-Bromo-3-(6-bromohexyl)thiophene (**5**) (14.0 g, 42.9 mmol) was dissolved into 140 mL of CH_2Cl_2 in a 300 mL round flask. After cooling the solution at 0 °C, iodobenzene diacetate (7.22 g, 22.4 mmol) and iodine (5.17 g, 40.8 mmol) were added and stirred overnight at 0 °C. The conversion of this reaction was carefully checked by ^{1}H NMR. If necessary, more iodobenzene diacetate and iodine with a molar ratio of 1.0 to 1.1 were added to achieve complete conversion of the starting material. The reaction mixture was poured into 10% $Na_2S_2O_3$(aq). The organic layer was sequentially washed with 10% $Na_2S_2O_3$(aq) once and with water twice. CH_2Cl_2 in the solution was evaporated after being dried with $MgSO_4$ and filtered; then, iodobenzene diacetate was removed by vacuum distillation. The residue was further purified by a short silica gel column with hexane as the eluent to obtain 2-bromo-5-iodo-3-(6-bromohexyl)thiophene (**6**) (18.0 g, 39.8 mmol) in 93% yield. ^{1}H NMR (500 MHz, $CDCl_3$): δ 6.96 (s, 1H), 3.41 (t, 2H), 2.53 (t, 2H), 1.86 (m, 2H), 1.56 (m, 2H), 1.46 (m, 2H), 1.34 (m, 2H).

(6,6)-Phenyl C_{61} Butyric Acid Propargyl Ester (PCBP) (10). (6,6)-Phenyl C_{61} butyric acid (**8**) was synthesized by following ref 31. CS_2 was distilled over CaH_2 prior to use. (6,6)-Phenyl C_{61} butyric acid (**8**) (200 mg, 0.22 mmol) was dissolved into 100 mL of CS_2 in a dried 200 mL two-necked round flask. After $SOCl_2$ (4 mL) was added by syringe, the reaction mixture was refluxed overnight under N_2. After removing the heating bath, CS_2 was evaporated in vacuum. NaH (26.8 mg, 1.1 mmol) and toluene (100 mL) were placed into another dried two-necked 100 mL round flask. Propargyl alcohol (62.5 mg, 1.1 mmol) was added to this suspension, and the reaction mixture was stirred for 1 h under N_2. This solution was transferred to the previous flask containing (6,6)-phenyl C_{61} butyryl chloride (**9**). The combined reaction mixture was stirred overnight at room temperature under N_2. The reaction mixture was poured into water, and the organic fraction was extracted with toluene. After washing the organic layer with water several times, toluene was evaporated. The residue was purified by silica gel column (eluent: hexane:$CHCl_3$ = 2:3) to obtain pure (6,6)-phenyl C_{61} butyric acid propargyl ester (PCBP) (**10**) (195 mg, 94% yield). ^{1}H NMR (500 MHz, $CDCl_3$): δ 7.93 (d, 2H), 7.55 (m, 2H), 7.47 (m, 1H), 4.69 (s, 2H), 2.93 (m, 2H), 2.58 (m, 2H), 2.48 (s, 1H), 2.21 (m, 2H).

Typical Procedure for the Model Fullerene-Attachment Reaction. (6,6)-Phenyl C_{61} butyric acid propargyl ester **10** (18.6 mg, 2.0 mmol), 1 mL of hexyl azide solution in toluene (38.2 mg mL^{-1}), and 14 mL of toluene were added to a 50 mL round flask. CuBr (1.0 mg, 7.0 mmol) and 1 drop of PMDETA were added to the solution. The reaction mixture was stirred at room temperature for 24 h and poured into MeOH. The solution was filtered, and the residue was washed with MeOH to obtain the product.

This reaction in air resulted in the formation of a bis-triazole byproduct $\mathbf{M_2}$ with low reaction conversion (around 50%), which seems to be due to oxidation of the Cu(I) catalyst. The reaction under N_2 and the use of distilled PMDETA (removing oxidized amine) completely suppressed the formation of the bis-triazole compound, and the reaction conversion reached 100%.

Poly[(3-(6-bromohexyl)thiophene)-*co*-(3-hexylthiophene)] (P3HT-*co*-P3BrHT) (B_R). 2-Bromo-5-iodo-3-hexylthiophene (**3**) (1.193 g, 3 mmol), 2-bromo-5-iodo-3-(6-bromohexyl)thiophene (**6**) (150 mg, 0.37 mmol), and 30 mL of anhydrous THF were added to a two-necked 50 mL round-bottom flask with a stirring bar. After cooling the flask at 0 °C, ^{i}Pr-MgCl (1.69 mL, 3.37 mmol) was then added to the flask via syringe. After the solution was stirred for 1 h at 0 °C, the cooling bath was removed and Ni(dppp)Cl_2 (13.0 mg, 0.024 mmol) was added in one portion. The mixture was stirred for 90 min at 35 °C, and then the reaction was quenched with 5 M HCl(aq). The polymer was extracted by $CHCl_3$ and sequentially washed with 2 M HCl(aq) twice, neutralized with $NaHCO_3$(aq), and washed with water twice. After $CHCl_3$ was evaporated, the residue was reprecipitated into MeOH. After filtration, the polymer was purified by Soxhlet extraction with MeOH and hexane, sequentially. The polymer was extracted by $CHCl_3$ and reprecipitated into MeOH. The suspension was filtered, and the residue was dried under vacuum to produce 425 mg of the product $\mathbf{B_R}$ in 72% yield. ^{1}H NMR (500 MHz, $CDCl_3$): 6.98 (s, 1H), 3.42 (t, 2H), 2.80 (t, 2H), 1.89 (t, 2H), 1.71 (m, 2H), 1.51 (m, 2H), 1.44 (m, 2H), 1.35 (m, 4H) 0.91 (t, 3H). Regioregularity (RR): head-to-tail ratio was determined as >97% by ^{1}H NMR. M_n = 22 600 and M_w/M_n = 1.11 determined by GPC.

Poly(3-hexylthiophene)-*b*-[3-hexylthiophene-*co*-3-(6-bromohexy)thiophene](P3HT-*b*-(P3HT-*co*-P3BrHT)) (B_1). 2-Bromo-5-iodo-3-hexylthiophene (746 mg, 2 mmol) and 20 mL of anhydrous THF were added to a two-necked 50 mL round-bottom flask with a stirring bar (flask A). After cooling the flask at 0 °C, *i*Pr-MgCl (1 mL, 2 mmol) was then added to the flask via syringe. The solution was stirred for 1 h at 0 °C, then the cooling bath was removed, and Ni(dppp)Cl_2 (8.3 mg, 0.015 mmol) was added in one portion. The mixture was stirred for 40 min at room temperature and then for 50 min at 35 °C. During this time, 2-bromo-5-iodo-3-hexylthiophene (149 mg, 0.4 mmol), 2-bromo-5-iodo-3-(6-

dx.doi.org/10.1021/ma300376m | *Macromolecules* 2012, 45, 6424−6437

bromohexyl)thiophene (180 mg, 0.4 mmol), and 10 mL of anhydrous THF were added to a two-necked 50 mL round-bottom flask (flask B) with a stirring bar. After cooling the flask at 0 °C, *i*Pr-MgCl (0.4 mL, 0.8 mmol) was added to flask B via syringe and stirred for 30 min. A small amount of the reaction mixture in flask A was taken out by syringe for GPC analysis. After this sampling, the reaction mixture in flask B was added to flask A via syringe and stirred at 35 °C for 3 h. The reaction mixture was quenched by adding 5 M HCl(aq), and some of reaction mixture was taken for GPC analysis. The purification of this reaction mixture was done by the same procedure as for P3HT-*co*-P3BrHT ($\mathbf{B_R}$), and 328 mg of the diblock copolymer $\mathbf{B_1}$ was obtained in 66% yield. ^{1}H NMR (500 MHz, $CDCl_3$): 6.98 (s, 1H), 3.42 (t, 2H), 2.80 (t, 2H), 1.89 (t, 2H), 1.71 (m, 2H), 1.52 (m, 2H), 1.44 (m, 2H), 1.35 (m, 4H) 0.91 (t, 3H). RR: >97% by ^{1}H NMR.

Poly(3-hexylthiophene)-*b*-[3-hexylthiophene-*co*-3-(6-bromohexy)thiophene](P3HT-*b*-(P3HT-*co*-P3BrHT)) ($\mathbf{B_2}$). Similar procedures to those for $\mathbf{B_1}$ with **3** (821 mg, 2.2 mmol) in flask A and the mixture of **3** (75 mg, 0.2 mmol) and **6** (180 mg, 0.4 mmol) in flask B produced 333 mg of the diblock copolymer $\mathbf{B_2}$ in 67% yield. ^{1}H NMR (500 MHz, $CDCl_3$): 6.98 (s, 1H), 3.41 (t, 2H), 2.80 (t, 2H), 1.89 (t, 2H), 1.71 (m, 2H), 1.52 (m, 2H), 1.44 (m, 2H), 1.35 (m, 4H) 0.91 (t, 3H). RR: >97% by ^{1}H NMR.

Poly(3-hexylthiophene)-*b*-3-(6-bromohexy)thiophene]-(P3HT-*b*-P3BrHT) ($\mathbf{B_3}$). Similar procedures to those for $\mathbf{B_1}$ with **3** (895 mg, 2.4 mmol) in flask A and **6** (225 mg, 0.5 mmol) in flask B produced 314 mg of the diblock copolymer $\mathbf{B_3}$ in 69% yield. ^{1}H NMR (500 MHz, $CDCl_3$): 6.98 (s, 1H), 3.42 (t, 2H), 2.80 (t, 2H), 1.89 (t, 2H), 1.71 (m, 2H), 1.52 (m, 2H), 1.44 (m, 2H), 1.35 (m, 4H) 0.91 (t, 3H). RR: >97% by ^{1}H NMR.

Poly[(3-(6-azidehexyl)thiophene)-*co*-(3-hexylthiophene)] (P3HT-*co*-P3N$_3$HT) ($\mathbf{C_R}$). Poly[(3-(6-bromohexyl)thiophene)-*co*-(3-hexylthiophene)] (P3HT-*co*-P3BrHT), $\mathbf{B_R}$ (120 mg), *n*-Bu_4NBr (1.29 g, 4 mmol), and 30 mL of toluene were added to a two-necked 100 mL round-bottom flask with a stirring bar. NaN_3 solution (1.0 g, 15.4 mmol in 15 mL of water) was added to the flask, and the solution was heated to reflux for 24 h. After the water layer was removed from the reaction mixture by syringe, a fresh mixture of NaN_3 (1.0 g, 15.4 mmol) and *n*-Bu_4NBr (322 mg, 1 mmol) in 15 mL of water was added again. The reaction mixture was refluxed for 24 h to complete the conversion of the bromohexyl group. The organic layer was extracted with toluene and washed with water several times. After concentrating the toluene solution by evaporation, the solution was precipitated into MeOH twice and hexane once. The solid residue was filtered and dried under vacuum to obtain the pure product $\mathbf{C_R}$ (107 mg) in 92% yield. This compound is best stored under vacuum or inert conditions with protection from light. ^{1}H NMR (500 MHz, $CDCl_3$): 6.98 (s, 1H), 3.28 (t, 2H), 2.80 (t, 2H), 1.71 (m, 2H), 1.63 (m. 2H), 1.44 (m, 2H), 1.35 (m. 4H), 0.91 (t, 3H).

Poly(3-hexylthiophene)-*b*-[3-hexylthiophene-*co*-3-(6-azidehexy)thiophene](P3HT-*b*-(P3HT-*co* P3N$_3$HT)) ($\mathbf{C_1}$). A similar procedure to that for $\mathbf{C_R}$ starting from 128 mg of $\mathbf{B_1}$ produced 117 mg of $\mathbf{C_1}$ in 94% yield. ^{1}H NMR (500 MHz, $CDCl_3$): 6.98 (s, 1H), 3.28 (t, 2H), 2.80 (t, 2H), 1.71 (m, 2H), 1.63 (m. 4H), 1.44 (m, 2H), 1.35 (m. 4H), 0.91 (t, 3H).

Poly(3-hexylthiophene)-*b*-[3-hexylthiophene-*co*-3-(6-azidehexy)thiophene](P3HT-*b*-(P3HT-*co* P3N$_3$HT)) ($\mathbf{C_2}$). A similar procedure to that for $\mathbf{C_R}$ starting from 124 mg of $\mathbf{B_2}$ produced 113 mg of $\mathbf{C_2}$ in 92% yield. ^{1}H NMR (500 MHz, $CDCl_3$): 6.98 (s, 1H), 3.28 (t, 2H), 2.80 (t, 2H), 1.71 (m, 2H), 1.63 (m. 2H), 1.44 (m, 2H), 1.35 (m. 4H), 0.91 (t, 3H).

Poly(3-hexylthiophene)-*b*-(3-(6-azidehexy)thiophene)-(P3HT-*b*-P3N$_3$HT) ($\mathbf{C_3}$). A similar procedure to that for $\mathbf{C_R}$ starting from 130 mg of $\mathbf{B_3}$ produced 118 mg of $\mathbf{C_3}$ in 93% yield. ^{1}H NMR (500 MHz, $CDCl_3$): 6.98 (s, 1H), 3.28 (t, 2H), 2.80 (t, 2H), 1.71 (m, 2H), 1.63 (m. 2H), 1.44 (m, 2H), 1.35 (m. 4H), 0.91 (t, 3H).

Poly[(3-hexylthiophene)-*co*-((3-hexylthiophene)-*graft*-PCBP)](P3HT-*co*-(P3HT-*graft*-PCBP)) ($\mathbf{D_R}$). PMDETA was purified by vacuum distillation and stored in a glovebox to prevent oxidation. CuBr was also stored in a glovebox. The synthesis was conducted under N_2. P3HT-*co*-P3N$_3$HT (34.3 mg) and PCBP **10** (41.2 mg, 0.044 mmol) were dissolved into 22 mL of *o*-xylene by heating in a 50 mL flask with a stirring bar. A solution of two drops of PMDETA and CuBr (1.4 mg, 0.01 mmol) in 8 mL of *o*-xylene was added to the polymer solution and stirred at room temperature for 24 h under protection from light. After the reaction, the mixture was poured into MeOH. The residue was filtered, redissolved into $CHCl_3$, and then precipitated to MeOH again. The residue was filtered, and a small amount of the compound was taken for GPC analysis. Unreacted fullerene derivative **10** in this compound was removed by using a preparative size exclusion column and $CHCl_3$ as the eluent. The fractionated solution was precipitated to hexane, and the residue was dried in vacuum to obtain the product (46.7 mg) in 85% yield. ^{1}H NMR (500 MHz, $CDCl_3$): δ 7.87 (d, 2H), 7.53 (s, 1H), 7.48 (m, 2H), 7.42 (m, 1H), 6.97 (s, 1H), 5.19 (s, 2H), 4.31 (t, 2H), 2.86 (t, 2H), 2.80 (t, 2H), 2.50 (t, 2H), 2.14 (t, 2H), 1.90 (t, 2H), 1.70 (m, 2H), 1.44 (m, 2H), 1.35 (m, 4H), 0.91 (t, 3H).

Poly(3-hexylthiophene)-*b*-(3-hexylthiophene-*graft*-PCBP)-(P3HT-*b*-(P3HT-*graft*-PCBP)) ($\mathbf{D_1}$). A similar procedure to that for $\mathbf{D_R}$ starting from 40 mg of $\mathbf{C_1}$ and 60 mg of PCBP **10** except for the reaction time (48 h), reaction temperature (50 °C), and total solvent amount ($\mathbf{C_1}$ in *o*-xylene with a concentration of 0.8 mg mL^{-1}), produced 52.3 mg of $\mathbf{D_1}$ in 82% yield. Unreacted fullerene derivative **10** was removed by precipitation to CH_2Cl_2 twice or by using a preparative size exclusion column and $CHCl_3$ as the eluent. It should be noted that an excess of PCBP **10** had to be used in this reaction; otherwise, a cross-linking fraction would be observed in the GPC chart (see main text). ^{1}H NMR (500 MHz, $C_2D_4Cl_4$, 100 °C): δ 7.86 (d, 2H), 7.5−7.4 (s, 1H), 7.47 (m, 2H), 7.40 (m, 1H), 6.97 (s, 1H), 5.16 (s, 2H), 4.26 (br, 2H), 2.89 (t, 2H), 2.81 (t, 2H), 2.49 (t, 2H), 2.13 (br, 2H), 1.88 (br, 2H), 1.70 (m, 2H), 1.43 (m, 2H), 1.35 (m, 4H), 0.91 (t, 3H).

Poly(3-hexylthiophene)-*b*-[3-hexylthiophene-*co*-3-(hexylthiophene-*graft*-PCBP)](P3HT-*b*-(P3HT-*co*-(P3HT-*graft*-PCBP))) ($\mathbf{D_2}$). A similar procedure to that for $\mathbf{D_1}$ starting from 40 mg of $\mathbf{C_2}$ and 72 mg of PCBP **10** produced 51.5 mg of $\mathbf{D_2}$ in 80% yield. ^{1}H NMR (500 MHz, $C_2D_4Cl_4$, 100 °C): δ 7.86 (d, 2H), 7.5−7.4 (s, 1H), 7.47 (m, 2H), 7.41 (m, 1H), 6.98 (s, 1H), 5.17 (s, 2H), 4.27 (br, 2H), 2.90 (t, 2H), 2.81 (t, 2H), 2.50 (t, 2H), 2.14 (br, 2H), 1.89 (br, 2H), 1.72 (m, 2H), 1.44 (m, 2H), 1.36 (m, 4H), 0.92 (t, 3H).

Poly(3-hexylthiophene-*b*-3-(hexylthiophene-*graft*-PCBP)-(P3HT-*b*-(P3HT-*graft*-PCBP)) ($\mathbf{D_3}$). A similar procedure to that for $\mathbf{D_1}$ starting from 40 mg of $\mathbf{C_3}$ and 96 mg of PCBP **10** produced 51 mg of $\mathbf{D_3}$ in 79% yield. ^{1}H NMR (500 MHz, $C_2D_4Cl_4$, 100 °C): δ 7.86 (d, 2H), 7.5−7.4 (s, 1H), 7.47 (m, 2H), 7.40 (m, 1H), 6.97 (s, 1H), 5.16 (s, 2H), 4.25 (br, 2H), 2.89 (t, 2H), 2.80 (t, 2H), 2.49 (t, 2H), 2.13 (br, 2H), 1.88 (br, 2H), 1.71 (m, 2H), 1.43 (m, 2H), 1.35 (m, 4H), 0.91 (t, 3H).

Measurements. Gel permeation chromatography (GPC) was performed on a Shimadzu Prominence system equipped with a UV detector and columns (TSK-gel G3000H$_{XL}$ and TSK-gel G5000$_{XL}$) using $CHCl_3$ as the eluent at 40 °C. The sample solutions were filtered by PTFE filter (pore size: 0.2 μm) before the injection. A Shimadzu Prominence semipreparative HPLC system with a UV detector was used for the purification of the fullerene attached copolymers. The conversion of the monomers were analyzed by analytical GC performed on a Focus GC-PolarisQ ion-trap type GC-MS (Thermo Scientific). Unreacted fullerene derivative **10** was removed from the fullerene attached copolymers by using preparative size exclusion column (Shimadzu GPC20025C, pore size: 6 μm) and $CHCl_3$ as the eluent at room temperature. The sample solutions were filtered by PTFE filter (pore size: 0.2 μm) before the injection. ^{1}H NMR (500 MHz) and ^{13}C NMR (125 MHz) spectra were measured on a JEOL Alpha FT-NMR spectrometer equipped with an Oxford superconducting magnet system. Matrix-assisted laser desorption/ionization time-of-flight mass spectrometry (MALDI-TOF-MS) was carried out on an Applied Biosystems BioPestrometry Workstation model Voyager DE-SSTR spectrometer in the reflection ion mode. UV−vis spectra and fluorescent spectra and FT-IR spectra were recorded on a JASCO V-650 spectrophotometer and IR Prestige-21 systems (Shimadzu), respectively. The FT-IR sample was prepared by drop-

dx.doi.org/10.1021/ma300376m | *Macromolecules* 2012, 45, 6424−6437

casting the polymer solution on a KBr substrate. The polymer film samples for UV−vis absorption measurement were prepared on a quartz substrate by spin-coating (600 rpm) from chlorobenzene solution (10 mg mL^{-1}). Tapping-mode atomic force microscopy (AFM) was performed on a Nanoscope III (Digital Instruments, Inc.). The polymer films for AFM measurements were prepared by spin-coating (600 rpm) from chlorobenzene solution (10 mg mL^{-1}) and annealed at 150 °C for 1 h. Differential scanning calorimetry (DSC) of the polymer bulk samples was performed on Rigaku DSC 8230 with a heating rate of 5 K min^{-1} under N_2 flow. The XRD diffraction patterns were recorded on a RIGAKU Smart lab X-ray diffractometer. The films for XRD measurement were prepared by spin-coating (600 rpm) the polymer solutions (11 mg mL^{-1} in the mixed solvent of chlorobenzene and $CHCl_3$ (3:2)) on a silicon substrate and annealed at 150 °C for 1 h. Cyclic voltammograms (CVs) were recorded on HSV-100 (Hokuto Denkou) potentiostat at a scan rate of 50 mV/s using Pt electrodes and an Ag/Ag^+ (0.01 M $AgNO_3$ and 0.1 M TBAP in acetonitrile) reference electrode in an anhydrous and nitrogen-saturated electrolyte solution (0.1 M Bu_4NPF_6 in CH_2Cl_2 or CH_3CN). HOMO and LUMO energy levels were determined from the oxidation and reduction onsets of the second scan from CV data, assuming that the half-wave potential of ferrocene corresponds to −4.8 eV.

Typical Procedure for Photovoltaic Device Preparation. Organic photovoltaic cells were prepared with the structure of ITO/PEDOT:PSS/active layer/Al. ITO-coated glass substrates were washed by ultrasonication sequentially in detergent, water, acetone, and 2-propanol. PEDOT:PSS was spin-coated on the ITO substrate at 3000 rpm. After drying the substrate under vacuum at 150 °C for 30 min, the substrates were transferred into the glovebox. The following procedure except the measurement of the device performance was all conducted in the glovebox.

Fullerene-attached copolymers (11 mg/mL) were dissolved into mixed solvent (chlorobenzene:$CHCl_3$ = 3:2) by stirring at 40 °C for several hours. After filtered by a PTFE filter (0.2 μm), the solution was spin-coated on the substrate at 500−1200 rpm. After drying the solvent, the substrate was transferred into an evaporation chamber (ALS technology H-2807 vacuum evaporation system with E-100 load lock). Al electrode (80 nm) was evaporated on substrate under high vacuum (10^{-4}−10^{-5} Pa). After the deposition, the device was thermally annealed on a hot plate. The measurement was conducted in air under the irradiation of AM 1.5 simulated solar light (100 mW cm^{-2}, Peccell Technologies PCE-L11). The irradiated area of the device was defined by a photomask as 0.06 cm^2. The current−voltage characteristics of the photovoltaic cells were measured using the Keithley 2400 *I*−*V* measurement system. Light intensity was adjusted by a standard silicon solar cell with an optical filter (Bunkou Keiki BS520).

■ ASSOCIATED CONTENT

Ⓢ Supporting Information

Synthesis, ^1H NMR, and IR spectra. This material is available free of charge via the Internet at http://pubs.acs.org.

■ AUTHOR INFORMATION

Corresponding Author

*E-mail: k-tajima@light.t.u-tokyo.ac.jp (K.T.); hashimoto@light.t.u-tokyo.ac.jp (K.H.).

Notes

The authors declare no competing financial interest.

■ ACKNOWLEDGMENTS

This work was supported in part by the Global COE Program (Chemistry Innovation through Cooperation of Science and Engineering).

■ REFERENCES

(1) Krebs, F. C. *Sol. Energy Mater. Sol. Cells* **2009**, *93*, 394.
(2) Peet, J.; Senatore, M. L.; Heeger, A. J.; Bazan, G. C. *Adv. Mater.* **2009**, *21*, 1521.
(3) Yu, G.; Gao, J.; Hummelen, J. C.; Wudl, F.; Heeger, A. J. *Science* **1995**, *270*, 1789.
(4) Hiramoto, M.; Fujiwara, H.; Yokoyama, M. *Appl. Phys. Lett.* **1991**, *58*, 1062.
(5) Liang, Y.; Wu, Y.; Feng, D.; Tsai, S.-T.; Son, H.-J.; Li, G.; Yu, L. *J. Am. Chem. Soc.* **2009**, *131*, 56.
(6) Liang, Y.; Yu, L. *Polym. Rev.* **2010**, *50*, 454.
(7) Yang, C.; Zhou, E.; Miyanishi, S.; Hashimoto, K.; Tojima, K. *ACS Appl. Mater. Interfaces* **2011**, *3*, 4053.
(8) Conings, B.; Bertho, S.; Vandewal, K.; Senes, A.; D'Haen, J.; Manca, J.; Janssen, R. A. J. *Appl. Phys. Lett.* **2010**, *96*, 163301.
(9) Roncali, J. *Chem. Soc. Rev.* **2005**, *34*, 483.
(10) Segura, J. L.; Martin, N.; Guldi, D. M. *Chem. Soc. Rev.* **2005**, *34*, 31.
(11) Bu, L. J.; Guo, X. Y.; Yu, B.; Qu, Y.; Xie, Z. Y.; Yan, D. H.; Geng, Y. H.; Wang, F. S. *J. Am. Chem. Soc.* **2009**, *131*, 13242.
(12) Nishizawa, T.; Lim, H. K.; Tajima, K.; Hashimoto, K. *Chem. Commun.* **2009**, 2469.
(13) Nishizawa, T.; Tajima, K.; Hashimoto, K. *J. Mater. Chem.* **2007**, *17*, 2440.
(14) Neuteboom, E. E.; Meskers, S. C. J.; van Hal, P. A.; van Duren, J. K. J.; Meijer, E. W.; Janssen, R. A. J.; Dupin, H.; Pourtois, G.; Cornil, J.; Lazzaroni, R.; Bredas, J. L.; Beljonne, D. *J. Am. Chem. Soc.* **2003**, *125*, 8625.
(15) Cravino, A.; Sariciftci, N. S. *J. Mater. Chem.* **2002**, *12*, 1931.
(16) Sommer, M.; Lang, A. S.; Thelakkat, M. *Angew. Chem., Int. Ed.* **2008**, *47*, 7901.
(17) Tan, Z.; Hou, J. H.; He, Y. J.; Zhou, E. J.; Yang, C. H.; Li, Y. F. *Macromolecules* **2007**, *40*, 1868.
(18) Ouhib, F.; Khoukh, A.; Ledeuil, J. B.; Martinez, H.; Desbrieres, J.; Dagron-Lartigau, C. *Macromolecules* **2008**, *41*, 9736.
(19) Stalmach, U.; de Boer, B.; Videlot, C.; van Hutten, P. F.; Hadziioannou, G. *J. Am. Chem. Soc.* **2000**, *122*, 5464.
(20) Lee, J. U.; Cirpan, A.; Emrick, T.; Russell, T. P.; Jo, W. H. *J. Mater. Chem.* **2009**, *19*, 1483.
(21) Yang, C.; Lee, J. K.; Heeger, A. J.; Wudl, F. *J. Mater. Chem.* **2009**, *19*, 5416.
(22) Ramos, A. M.; Rispens, M. T.; van Duren, J. K. J.; Hummelen, J. C.; Janssen, R. A. J. *J. Am. Chem. Soc.* **2001**, *123*, 6714.
(23) Roncali, J. *Adv. Energy Mater.* **2011**, *1*, 147.
(24) Mulherin, R. C.; Jung, S.; Huettner, S.; Johnson, K.; Kohn, P.; Sommer, M.; Allard, S.; Scherf, U.; Greenham, N. C. *Nano Lett.* **2011**, *11*, 4846.
(25) Barrau, S.; Heiser, T.; Richard, F.; Brochon, C.; Ngov, C.; van de Wetering, K.; Hadziioannou, G.; Anokhin, D. V.; Ivanov, D. A. *Macromolecules* **2008**, *41*, 2701.
(26) Zhang, W. B.; Tu, Y.; Ranjan, R.; Van Horn, R. M.; Leng, S.; Wang, J.; Polce, M. J.; Wesdemiotis, C.; Quirk, R. P.; Newkome, G. R.; Cheng, S. Z. D. *Macromolecules* **2008**, *41*, 515.
(27) Miyanishi, S.; Zhang, Y.; Tajima, K.; Hashimoto, K. *Chem. Commun.* **2010**, *46*, 6723.
(28) Rostovtsev, V. V.; Green, L. G.; Fokin, V. V.; Sharpless, K. B. *Angew. Chem., Int. Ed.* **2002**, *41*, 2596.
(29) Binder, W. H.; Sachsenhofer, R. *Macromol. Rapid Commun.* **2008**, *29*, 952.
(30) Wu, P.; Feldman, A. K.; Nugent, A. K.; Hawker, C. J.; Scheel, A.; Voit, B.; Pyun, J.; Frechet, J. M. J.; Sharpless, K. B.; Fokin, V. V. *Angew. Chem., Int. Ed.* **2004**, *43*, 3928.
(31) Hummelen, J. C.; Knight, B. W.; Lepeq, F.; Wudl, F.; Yao, J.; Wilkins, C. L. *J. Org. Chem.* **1995**, *60*, 532.
(32) Wei, Q. S.; Nishizawa, T.; Tajima, K.; Hashimoto, K. *Adv. Mater.* **2008**, *20*, 2250.
(33) Miyakoshi, R.; Yokoyama, A.; Yokozawa, T. *J. Am. Chem. Soc.* **2005**, *127*, 17542.
(34) Iovu, M. C.; Sheina, E. E.; Gil, R. R.; McCullough, R. D. *Macromolecules* **2005**, *38*, 8649.

(35) Zhang, Y.; Tajima, K.; Hirota, K.; Hashimoto, K. *J. Am. Chem. Soc.* **2008**, *130*, 7812.
(36) Zhang, Y.; Tajima, K.; Hashimoto, K. *Macromolecules* **2009**, *42*, 7008.
(37) Miyanishi, S.; Tajima, K.; Hashimoto, K. *Macromolecules* **2009**, *42*, 1610.
(38) Zhai, L.; Pilston, R. L.; Zaiger, K. L.; Stokes, K. K.; McCullough, R. D. *Macromolecules* **2003**, *36*, 61.
(39) Zhang, Y.; Tajima, K.; Hashimoto, K. *Synth. Met.* **2011**, *161*, 225.
(40) Miyakoshi, R.; Yokoyama, A.; Yokozawa, T. *Macromol. Rapid Commun.* **2004**, *25*, 1663.
(41) Angell, Y.; Burgess, K. *Angew. Chem., Int. Ed.* **2007**, *46*, 3649.
(42) Prato, M.; Li, Q. C.; Wudl, F.; Lucchini, V. *J. Am. Chem. Soc.* **1993**, *115*, 1148.
(43) Kamijo, S.; Jin, T.; Huo, Z. B.; Yamamoto, Y. *J. Org. Chem.* **2004**, *69*, 2386.
(44) Hawker, C. J. *Macromolecules* **1994**, *27*, 4836.
(45) Benanti, T. L.; Kalaydjian, A.; Venkataraman, D. *Macromolecules* **2008**, *41*, 8312.
(46) Brown, P. J.; Thomas, D. S.; Kohler, A.; Wilson, J. S.; Kim, J. S.; Ramsdale, C. M.; Sirringhaus, H.; Friend, R. H. *Phys. Rev. B* **2003**, *67*, 064203.
(47) Malow, M.; Wehrstedt, K. D.; Neuenfeld, S. *Tetrahedron Lett.* **2007**, *48*, 1233.
(48) Yu, X.; Yang, H.; Wu, S.; Geng, Y.; Han, Y. *Macromolecules* **2012**, *45*, 266.
(49) Liu, J. S.; Sheina, E.; Kowalewski, T.; McCullough, R. D. *Angew. Chem., Int. Ed* **2001**, *41*, 329.
(50) Zhang, Q.; Cirpan, A.; Russell, T. P.; Emrick, T. *Macromolecules* **2009**, *42*, 1079.
(51) Verduzco, R.; Botiz, I.; Pickel, D. L.; Kilbey, S. M., II; Hong, K.; Dimasi, E.; Darling, S. B. *Macromolecules* **2011**, *44*, 530.
(52) Dante, M.; Yang, C.; Walker, B.; Wudl, F.; Nguyen, T.-Q. *Adv. Mater.* **2010**, *22*, 1835.
(53) Campoy-Quiles, M.; Ferenczi, T.; Agostinelli, T.; Etchegoin, P. G.; Kim, Y.; Anthopoulos, T. D.; Stavrinou, P. N.; Bradley, D. D. C.; Nelson, J. *Nat. Mater.* **2008**, *7*, 158.
(54) Stevens, D. M.; Qin, Y.; Hillmyer, M. A.; Frisbie, C. D. *J. Phys. Chem. C* **2009**, *113*, 11408.
(55) Guo, J.; Ohkita, H.; Yokoya, S.; Benten, H.; Ito, S. *J. Am. Chem. Soc.* **2010**, *132*, 9631.
(56) Clarke, T. M.; Durrant, J. R. *Chem. Rev.* **2010**, *110*, 6736.
(57) Vandewal, K.; Tvingstedt, K.; Gadisa, A.; Inganas, O.; Manca, J. V. *Nat. Mater.* **2009**, *8*, 904.
(58) Veldman, D.; Meskers, S. C. J.; Janssen, R. A. J. *Adv. Funct. Mater.* **2009**, *19*, 1939.
(59) Vandewal, K.; Gadisa, A.; Oosterbaan, W. D.; Bertho, S.; Banishoeib, F.; Van Severen, I.; Lutsen, L.; Cleij, T. J.; Vanderzande, D.; Manca, J. V. *Adv. Funct. Mater.* **2008**, *18*, 2064.
(60) Holcombe, T. W.; Norton, J. E.; Rivnay, J.; Woo, C. H.; Goris, L.; Piliego, C.; Griffini, G.; Sellinger, A.; Bredas, J.-L.; Salleo, A.; Frechet, J. M. J. *J. Am. Chem. Soc.* **2011**, *133*, 12106.
(61) Tada, A.; Geng, Y.; Wei, Q.; Hashimoto, K.; Tajima, K. *Nat. Mater.* **2011**, *10*, 450.
(62) Izawa, S.; Hashimoto, K.; Tajima, K. *Chem. Commun.* **2011**, *47*, 6365.